Global Scientific JOURNALS

GSJ: Volume 8, Issue 12, December 2020, Online: ISSN 2320-9186
www.globalscientificjournal.com

Control of 8 DOF vehicle model suspension system by designing Second order SMC Controller

Yibeltal Antehunegn [1, †], Bisrat Yoseph (PhD) [2], Mebaye Belete [1]

[1] *AddisAbaba science and technology university, Ethiopia*

[2] *Defence College, Debrezeit, Ethiopia*

† *Corresponding Author: Tel: +251918562824 ; Email : yibeltal.antehunegn@aastu.edu.et*

***Abstract*—**In this paper the mathematical modeling of 8 DOF full car model active suspension system (ASS) using Lagrange formalism and design of Non-linear Control strategy, Second-Order Sliding Mode Control (SOSMC), based on a Super Twisting Algorithm (STA) has been proposed for ride quality and vehicle handling. MATLAB/Simulink software is used to simulate the work. The controlled parameters are sprung masses of driver set heave, vehicle's body heave, rolling and pitching displacements and unsprung masses of four wheels heave displacements. Its performance is evaluated compared to its corresponding passive suspension system (PSS). Three bump sinusoidal roads input is used for simulation. Finally, the performance of the proposed controller was demonstrated in the simulation study. The simulation shows excellent modeling and control performance is developed.

***Index Terms*—** **Active suspension**, **SOSMC, STA**, **Lagrange**, **8 DOF**, **MATLAB/Simulink.**

1. INTRODUCTION

When designing new vehicle systems, the automotive industry faces challenges to the ever-increasing improvement requirements relating to drive dynamics, ride comfort and driving safety. As well, environmental friendliness and energy efficiency are become important issues that customers cogitate when buying a new car. These demands can be fulfilled by evolving more effective control systems of drive dynamics, such as active suspension systems.

The main task of suspension system is the regulation of ride quality and vehicle handling. Regulation of ride quality refers to isolate passenger's body and cargos from road and inertial disturbances during braking, cornering and acceleration. Regulation of vehicle handling refers to produce sufficient contact between the tires and road by preventing suspension movements.

The suspension system is mainly categorized into three types: passive, semi-active and active. Passive suspension is the least complex system and has numerous advantages. But, the disadvantage of passive suspension is the limits of overcoming unwanted vibration that occurs due to road abnormalities [1,2]. Under normal parameters, passive performance is confined as it includes fixed spring and damper. Similarly, its efficiency depends on the fixed standard of certain automobile parameters [3]. Thus, to achieve better performance results, semi-active suspension uses the conventional spring and externally controlled damper [1]. In this type, the damping coefficient can be controlled based on the inputs from chassis motion sensor that measures the motion of the vehicle. The active suspension system uses actuators force elements in a closed loop control system alongside conventional passive suspension system [4]. The actuator force provides adequate control force to the system based on the input from the various sensors associated with it. The researchers have proposed the various control systems to enhance the active suspension system performance.

The PID control has been designed and analyzed for two DOF quarter car ASS [5]. The comparative of Fuzzy control and Linear Quadratic Gaussian (LQG) control have been proposed and investigated for two DOF quarter car model of ASS [6]. ASS of 4 DOF half car model using Fuzzy control systems and LQR have been analyzed [7]. ASS of 4 DOF half car model using proportional integral sliding control system has been proposed and analyzed [8]. Modeling and control of half car model by designing fuzzy control system has been analyzed on vehicle suspension models [9]. The full ASS modeling and design of Fractional Order Proportional Integral Derivative (FOPID) has been proposed and analyzed the performances of the system [10].

The modeling of 6 DOF half car model and design of ANFIS has been proposed and analyzed its performance by compared to PSS [11]. The mathematical model of 7 DOF car model by designing H ∞ controller was studied [12]. Its performance is compared to LQG controller simulations result. The result

shows that the H ∞ controller more robust stability and better performance than LQR. Modeling and control of quarter vehicle model by designing Fractional order sliding mode controller (FOSMC), Integral super twisting algorithm (ISMC), and Higher order sliding mode controller (HOSMC) were conducted [4]. The designed controllers were compared with LQR, PID, and PSS. The co-simulation result shows that the Super twisting algorithm (STA) based HOSMC has the capacity to reduce the road abnormalities that affect vehicle stability and provides better control performance to ISMC, FOSMC, PID, LQR, and PSS. However, full vehicle motion is not studied. The mathematical model of quarter car model using HOSMC was studied [2]. For comparison purposes first-order sliding mode controller (SMC) was designed. The result shows that the best performance was achieved by the HOSMC than first order SMC. Moreover, HOSMC controller used less control effort with less chattering than the first-order SMC, and it is preferable since high chattering may harm the actuator and other mechanical components of the system.

In summary, many studies on active suspensions, have been devoted on to simplified two degree of freedom quarter car models, with only studies few about over all motion control of full vehicle. Lately, even if few researchers have been done to full dynamic control of the vehicle, the implemented controllers lacked the robustness to system parameters changes.

To overcome the above problems this research is giving attention to full dynamic model of a vehicle and robust controller design. So, a full car model including driver set dynamics suspension system is developed, and a robust SOSMC controller is designed with a super twisting algorithm.

The paper is organized into five sections. In section 1, it introduces the vehicle suspension system. In Section 2, it develops the mathematical models. In Section 3, it designs second-order SMC based on the super twisting algorithm. In Section 4, it presents the simulation results, obtained from the control implementation of the mathematical model in the Simulink environment. Finally, in Section 5, it shows the control inputs and then concludes the work.

2. MATHEMATICAL MODELLING

In this section, a complete mathematical model for 8 DOF of vehicle model suspension system using Lagrange equation has been formulated and derived.

2.1. Lagrange equation

The ASS of a mathematical model is derived using simpler and more practical Lagrange equation [13] motion, for a mechanical system having n DOF can be given in equation 2.1. Where K is the kinetic energy, V is the potential energy, and D is the energy dissipation function of the system, q_r is the generalized rth coordinate, $\dot{q}_r$ is the velocity on rth coordinate and f_r is the actuator force on the mass m_r.

$$\frac{d}{dt}\frac{\partial K}{\partial \dot{q}_r} - \frac{\partial K}{\partial q_r} + \frac{\partial D}{\partial \dot{q}_r} + \frac{\partial V}{\partial q_r} = f_r, \quad r = 1,2,\ldots,n \qquad 2.1$$

For simplification, the following assumptions are considered for the derivations of the mathematical model.

- Vehicle's body is considered as rigid.
- The vehicle body can heave, roll and pitch
- The driver set and four vehicle wheels can only heave.
- All components are considered as linear.
- Small displacements are considered.
- Ground contact of vehicle is maintained continuously

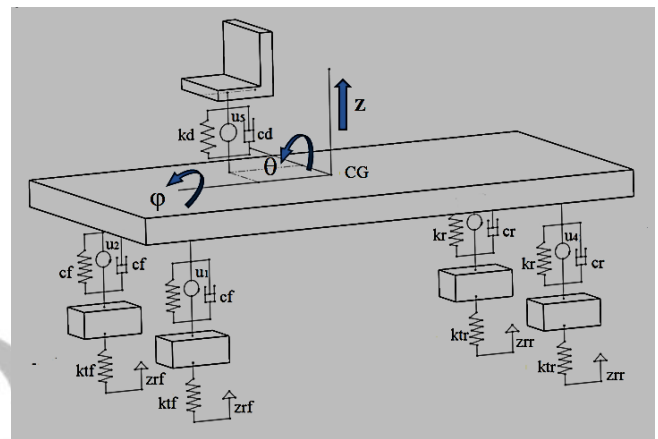

Figure 2.1. The 8 DOF vehicle model suspension systems

Where,

kd	Spring stiffness of driver's seat suspension
kf	Front spring stiffness of the suspension
kr	Rear spring stiffness of the suspension
cd	Damping coefficient of driver's set
cf	Front damper coefficient of the suspension
cr	Rear damper coefficient of the suspension
ktf	Front spring stiffness of the tyre
ktr	Rear spring stiffness of the tyre
CG	Center of gravity
zcg	Vertical motion of CG of vehicle body
φ	Roll motion of vehicle body at CG
θ	Pitch motion of vehicle body at CG
zrf	Road in put to front left and right wheel
zrr	Road in put to rear right and left wheel respectively
u5	Actuator force in driver body suspension system

u1, u2 Actuator force in the front left and right suspension system respectively

u3, u4 Actuator force in the rear right and left suspension system respectively

Based on the physical model of a vehicle as given in figure 3.1, the total kinetic energy (KE) of system is the sum of the translational KE of the driver seat, translational KE of a vehicle body, the rotational KE of a vehicle body and translational KE of all wheels, that is,

$$K = \begin{pmatrix} \frac{1}{2} m_d \dot{z}_d^2 + \frac{1}{2} m_v \dot{z}_{cg}^2 + \frac{1}{2} I_{xx} \dot{\varphi}^2 + \frac{1}{2} \\ I_{yy} \dot{\theta}^2 + \frac{1}{2} m_f \left(\dot{z}_1^2 + \dot{z}_2^2 \right) + \frac{1}{2} m_r \\ \left(\dot{z}_3^2 + \dot{z}_4^2 \right) \end{pmatrix} \quad 2.2$$

Based on the physical model of a vehicle, the total potential energy (PE) of the system, , is the sum of translational PE of the driver seat, translational PE of a vehicle body, the rotational PE of a vehicle body and translational PE of all wheels, that is,

$$V = \begin{pmatrix} \frac{1}{2} K_d (z_d - z_{cg} - f\varphi - e\theta)^2 + \frac{1}{2} k_f \\ (z_{cg} - z_1 + c\varphi - a\theta)^2 + \frac{1}{2} k_f \\ (z_{cg} - z_2 - d\varphi - a\theta)^2 + \frac{1}{2} k_r \\ (z_{cg} - z_3 - d\varphi + b\theta)^2 + \frac{1}{2} k_r \\ (z_{cg} - z_4 + c\varphi + b\theta)^2 + \frac{1}{2} k_{tf} \\ (z_1 - z_{r1})^2 + \frac{1}{2} k_{tf} (z_2 - z_{r2})^2 + \\ \frac{1}{2} k_{tr} (z_3 - z_{r3})^2 + \frac{1}{2} k_{tr} (z_4 - z_{r4})^2 \end{pmatrix} \quad 2.3$$

Based on the physical model of a vehicle, the total dissipation energy of the systems of the damper, D, is the sum of dissipated energy associated with suspension system connects the driver seat to the vehicle body and dissipated energy associated with suspension system connects the vehicle body to the four vehicle wheels, that is,

$$D = \begin{pmatrix} \frac{1}{2} c_d (\dot{z}_d - \dot{z}_{cg} - f\dot{\varphi} - e\dot{\theta})^2 + \frac{1}{2} c_f \\ (\dot{z}_{cg} - \dot{z}_1 + c\dot{\varphi} - a\dot{\theta})^2 + \frac{1}{2} c_f \\ (\dot{z}_{cg} - \dot{z}_2 - d\dot{\varphi} - a\dot{\theta})^2 + \frac{1}{2} c_r \\ (\dot{z}_{cg} - \dot{z}_3 - d\dot{\varphi} + b\dot{\theta})^2 + \frac{1}{2} c_r \\ (\dot{z}_{cg} - \dot{z}_4 + c\dot{\varphi} + b\dot{\theta})^2 \end{pmatrix} \quad 2.4$$

To obtain the equations of motion, we will apply 2.2, 2.3 and 2.4 to the Lagrange equation 2.1. Then, we get the following eight equations describing the dynamics of vehicle active suspension system.

For driver set heave motion:

$$m_d \ddot{z}_d = \begin{pmatrix} -c_d \dot{z}_d + c_d \dot{z}_{cg} + c_d f \dot{\varphi} + c_d e \dot{z}_d \theta - \\ k_d z_d + k_d z_{cg} + k_d f \varphi + k_d e\theta + u_5 \end{pmatrix} \quad 2.5$$

For vehicle body bounce motion:

$$m_v \dot{z}_{cg} = \begin{pmatrix} c_d \dot{z}_d - \left(c_d + 2\left(c_f + c_r\right)\right) \dot{z}_{cg} - \\ \left(c_d f + (c-d)\left(c_f + c_r\right)\right) \dot{\varphi} - \\ \left(c_d e + 2\left(c_r b - c_f a\right)\right) \dot{\theta} + \\ k_d z_d - \left(k_d + 2\left(k_f + k_r\right)\right) z_{cg} - \\ k_d f \varphi - \left((c-d)\left(k_f + k_r\right)\right) \varphi \\ -\left(k_d e + 2\left(k_r b - k_f a\right)\right) \theta + c_f \\ \dot{z}_1 + k_f z_1 + c_f \dot{z}_2 + k_f z_2 + c_r \dot{z}_3 \\ + k_r z_3 + c_r \dot{z}_4 + k_r z_4 + u_1 + u_2 + \\ u_3 + u_4 - u_5 \end{pmatrix} \quad 2.6$$

For vehicle body rolling motion:

$$I_{xx}\ddot{\varphi}=\begin{pmatrix} c_d f\dot{z}_d-\left(c_d f+(c-d)\left(c_f+c_r\right)\right)\\ \dot{z}_{cg}-(c_d f^2+(c^2+d^2)\left(c_f+c_r\right))\\ \dot{\varphi}-c_d fe\dot{\theta}-(c-d)(c_r b-c_f a)\dot{\theta}\\ +k_d fz_d-k_d fz_{cg}-(c-d)\left(k_f+k_r\right)\\ z_{cg}-k_d f^2\varphi-(c^2+d^2)\left(k_f+k_r\right)\varphi\\ -\left(k_d fe+(c-d)\left(k_r b-kfa\right)\right)\theta+\\ c_f c\dot{z}_1-c_f d\dot{z}_2-c_r d\dot{z}_3+c_r c\dot{z}_4+k_f\\ cz_1-k_f dz_2-k_r dz_3+k_r cz_4+cu_1-\\ du_2-du_3+cu_4+fu_5 \end{pmatrix} \quad 2.7$$

For vehicle body pitching motion:

$$I_{yy}\ddot{\theta}=\begin{pmatrix} c_d e\dot{z}_d-\left(c_d e+2\left(c_r b-c_f a\right)\right)\dot{z}_{cg}-\\ \left(c_d ef+(c-d)\left(c_r b-c_f a\right)\right)\dot{\varphi}-\\ (C_d e^2+2\left(C_f a^2+C_r b^2\right))\dot{\theta}+K_d e\\ Z_d-\left(k_d e+2\left(k_r b-k_f a\right)\right)z_{cg}-\\ \left(k_d ef+(c-d)\left(k_r b-k_f a\right)\right)\varphi-\\ (k_d e^2+2\left(k_f a^2+k_r b^2\right))\theta-c_f a\\ \dot{z}_1-c_f a\dot{z}_2+c_r b\dot{z}_3+c_r b\dot{z}_4-k_f az_1\\ -k_f az_2+k_r bz_3+k_r bz_4-au_1-au_2\\ +bu_3+bu_4+eu_5 \end{pmatrix} \quad 2.8$$

For front left wheel:

$$m_1\ddot{z}_1=\begin{pmatrix} c_f\dot{z}_{cg}-c_f\dot{z}_1+c_f c\dot{\varphi}-c_f a\dot{\theta}+k_f\\ z_{cg}-(k_f+k_{tf})z_1+k_f c\varphi-k_f a\\ \theta+k_{tf}z_{r1}-u_1 \end{pmatrix} \quad 2.9$$

For front right wheel:

$$m_2\ddot{z}_2=\begin{pmatrix} c_f\dot{z}_{cg}-c_f\dot{z}_2-c_f d\dot{\varphi}-c_f a\dot{\theta}+k_f\\ z_{cg}-(k_f+k_{tf})z_2-k_f d\varphi-k_f a\\ \theta+k_{tf}z_{r2}-u_2 \end{pmatrix} \quad 2.10$$

For rear right wheel:

$$m_3\ddot{z}_3=\begin{pmatrix} c_r\dot{z}_{cg}-c_r\dot{z}_3-c_r d\dot{\varphi}+c_r b\dot{\theta}+k_r\\ z_{cg}-(k_r+k_{tr})z_3-k_r d\varphi+k_r b\\ \theta+k_{tr}z_{r3}-u_3 \end{pmatrix} \quad 2.11$$

For rear left wheel:

$$m_4\ddot{z}_4=\begin{pmatrix} c_r\dot{z}_{cg}-c_r\dot{z}_4+c_r c\dot{\varphi}+c_r b\dot{\theta}+k_r\\ z_{cg}-\left(k_r+k_{tr}\right)z_4+k_r c\varphi+k_r b\\ \theta+k_{tr}z_{r4}-u_4 \end{pmatrix} \quad 2.12$$

2.2. State space model for active suspension system

The model can be written in the following state space form

$$\dot{x}(t)=Ax(t)+Bu(t)+f(x,t) \quad 2.13$$

Where $x(t)\in\Re^n$ is the state vector, $u(t)\in\Re^m$ is the control input, and the continuous function $f(x,t)$ represents the uncertainties with the mismatched Condition.

3. CONTROL SYSTEM DESIGN

3.1. Second Order Sliding Mode Controller

3.1.1. Super-twisting algorithm

Consider once more the dynamical system of relative degree 1 [2] and suppose that

$$\dot{\sigma}=h(t,x)+g(t,x)u \quad 3.1$$

Furthermore, assume that for some positive constants C, K_M, K_m, U_M, q

$$\left|\dot{h}\right|+U_M\left|\dot{g}\right|\le C, 0\le K_m\le g(t,x)\le K_M, \left|\frac{h}{g}\right|<qU_M, \quad 3.2$$

$$0<q<1$$

Then the control signal becomes

$$U=-\lambda|\sigma|^{\frac{1}{2}}\,sign(\sigma)+u \qquad \dot{u}=\begin{cases} -u, for\ |u|>U_M\\ -\alpha sign(\sigma), for\ |u|<U_M \end{cases} \quad 3.3$$

Theorem: [14] with $K_m\alpha > C$ and λ sufficiently large, the controller (3.3) guarantees the appearance of a 2-sliding mode $\sigma = \dot{\sigma} = 0$ in the system, which attracts the trajectories in finite time. The control u enters in a finite time segment $[-U_M, U_M]$ and stays there. It never leaves the segment, if the initial value is inside at the beginning. A sufficient (very crude!) condition for the validity of the theorem is

$$\lambda > \frac{\sqrt{\frac{2}{(K_m\alpha - C)}}(K_m\alpha + C)K_M(1+q)}{K_m^2(1-q)} \qquad 3.4$$

3.4 Calculated Controller parameters for regulation

The controller parameters listed below in Table 1 are calculated based on the above theorem.

Table 3.1. The calculated SOSMC controller parameters.

Variables/states	λ for Super-twisting SMC	α for Super-twisting SMC
z_d	200	0.003
z_{cg}	200	0.003
φ	200	0.003
θ	200	0.003
z_1	1	0.003
z_2	1	0.003
z_3	1	0.003
z_4	1	0.003

4. SIMULATION AND RESULT ANALYSIS

In this section, numerical simulations are carried out on the 8 DOF model ASS to validate the control performance of the proposed sliding mode control. For simulation purposes, the vehicle parameters are given in the appendix A table 1. The simulation is done by Matlab\Simulink software. The solver is Euler with fixed step size 0.01.

4.1 Comparative performance of ASS to PSS simulation for three bump Sinusoidal road input

These simulations are implemented for checking the effectiveness of the ASS over PSS at three bump road profile. The three bumps sinusoidal road profile is presented below where a denotes the bump amplitude and its value 0.005 m is taken [13]. The front left wheel and front right wheel reach the bumps at the same time as well as the rear left wheel and rear right wheel reach the bumps at the same time. The sinusoidal bump with frequency of 8 HZ has been characterized by

Three bump Sinusoidal roads input with frequency of 8 HZ has been characterized by

$$Z_{rf}(t) = \begin{cases} a(1-\cos 8\pi t) & 0.5s \le t \le 0.75s \\ \frac{a(1-\cos 8\pi t)}{2} & 3.0s \le t \le 3.25s \\ a(1-\cos 8\pi t) & 5.0s \le t \le 5.25s \\ 0 & Otherwise \end{cases} \qquad 4.1$$

$$Z_{rr}(t) = \begin{cases} a(1-\cos 8\pi t) & 3.5s \le t \le 3.25s \\ \frac{a(1-\cos 8\pi t)}{2} & 3.5s \le t \le 3.75s \\ a(1-\cos 8\pi t) & 7.5s \le t \le 7.75s \\ 0 & Otherwise \end{cases} \qquad 4.2$$

Equation 4.1 is an input disturbance for front right and left wheel and equation 4.2 is an input disturbance for rear right and left wheel.

4.1.1. Sprung mass displacements

In figure 4.1, 4.2, 4.3 and 4.4 shows the comparative performance of ASS and PSS for the parameters of driver set heave, vehicle body heave, roll, and pitch displacements respectively. As we see from the simulation graph, the peak to peak amplitude displacement for PSS is much larger than ASS for all states of the system. The comparative performance of ASS to PSS also studied under peak to peak displacement and settling time values. All controlled ASS states have above 90% improvement for both peak to peak and settling time than uncontrolled PSS states which are excellent performances. Their details peak to peak values and settling times are given in table 4.1 and table 4.2 respectively.

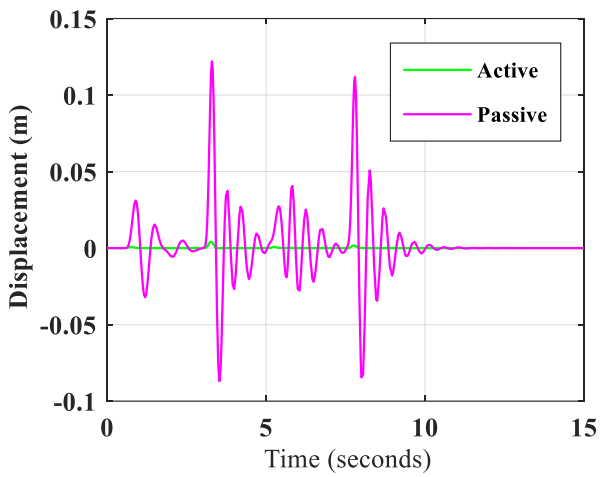

Figure 4.1. Driver set heave displacement simulations

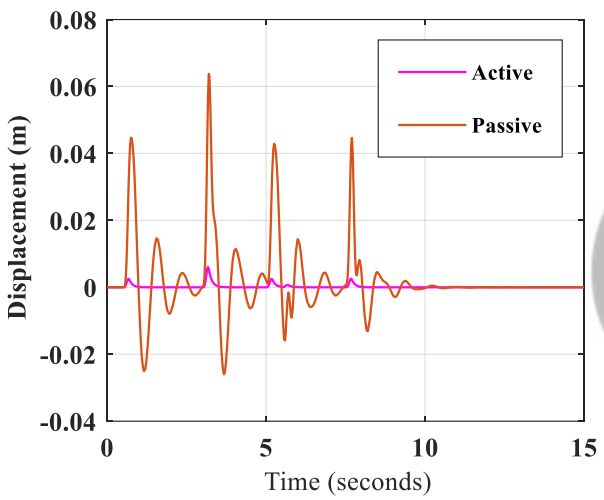

Figure 4.2. Vehicle body heave displacement simulations

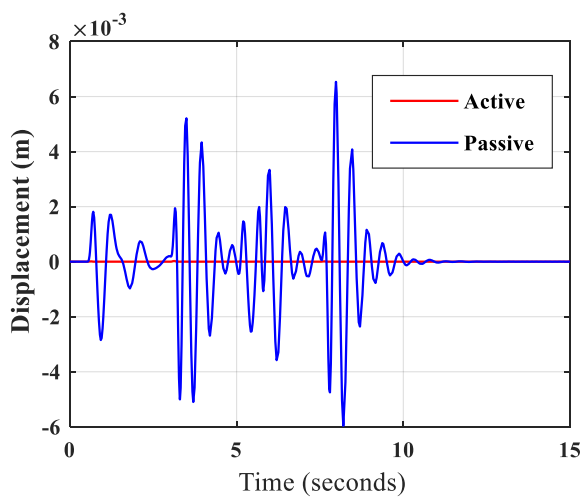

Figure 4.3. Vehicle body roll displacement simulations

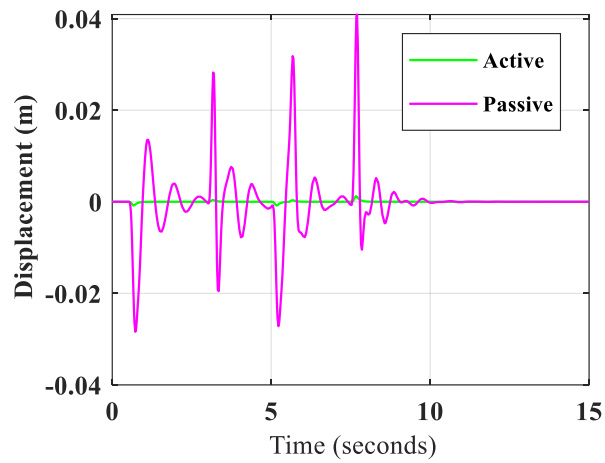

Figure 4.4. Vehicle body pitch displacement simulations

4.1.2. Unsprung mass displacements

In figure 4.5, 4.6, 4.7 and 5.8 shows the comparative performance of ASS and PSS for the parameters of front left heave, front right heave, rear right heave and rear left heave displacements respectively. As we see from the simulation graph, the peak to peak displacement for PSS is much larger than ASS for all states. The comparative performance of ASS to PSS measured under peak to peak displacement and settling time values. All controlled ASS states have above 75% and 71 % improvement for peak to peak and settling time respectively than uncontrolled PSS states which are best performances. Their details peak to peak values and settling times are given in table 4.1 and table 4.2 respectively.

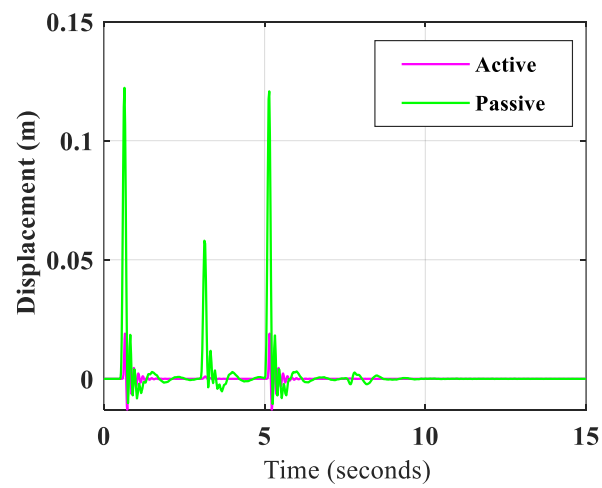

Figure 4.5. Front left wheel heave displacement simulations

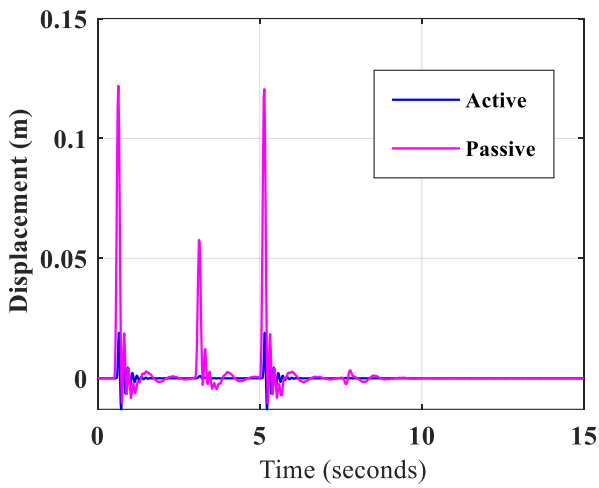

Figure 4.6. Front right wheel heave displacement simulations

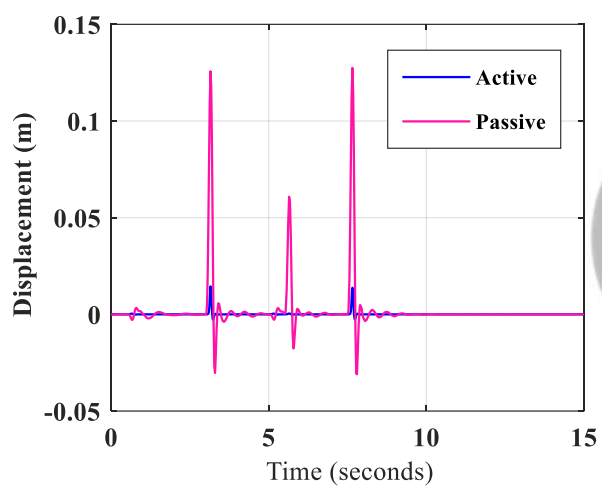

Figure 4.7. Rear right wheel heave displacement simulations

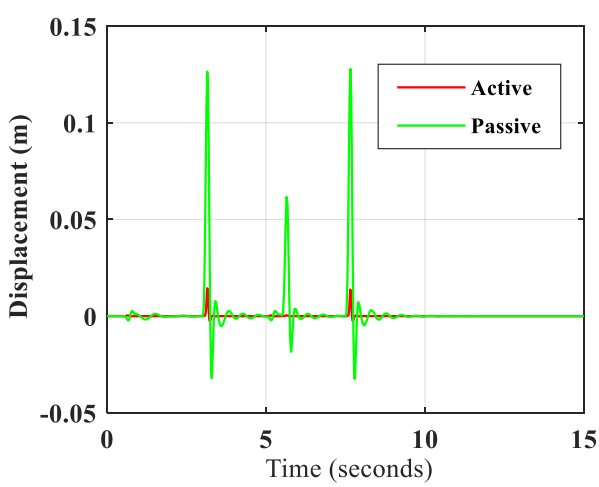

Figure 4.8. Rear left wheel heave displacement simulations

$$\textit{Improvement} = \frac{\text{PSS} - \text{ASS}}{\text{PSS}} * 100\%$$

Table 4.1. Comparison of peak-to-peak amplitude displacement of PSS and ASS for three-bump sinusoidal road input

Parameters	PSS (m)	ASS (m)	Improvement %
Driver's seat heave	0.2082	0.004255	97.9%
Vehicle's body heave	0.08928	0.006072	93.2%
Vehicle's body roll	0.01200	0.00002447	99.7%
Vehicle's body pitch	0.06928	0.002038	97.1%
Front left heave	0.1328	0.03193	75.9%
Front right heave	0.1326	0.03192	75.9%
Rear right heave	0.1576	0.01728	89.0%
Rear left heave	0.1599	0.01729	89.1%

Table 4.2. Comparison of settling time of PSS and ASS for three bump road profile

Parameters	ASS (sec)	PSS (sec)	Improvement
Driver's seat heave	2	10	80%
Vehicle's body heave	2	9.9	79%
Vehicle's body roll	2.1	10.5	80%
Vehicle's body pitch	2.1	10.5	80%
Front left heave	1.9	8	76%
Front right heave	1.9	8	76%
Rear right heave	2	8.75	77%
Rear left heave	2	8.75	77%

Summary

The comparisons of ASS to PSS have been studied under three bump road input disturbances. The mission of the controller is to bring the disturbance a vehicle motions to the equilibrium with a

small amplitude and short settle time. For example driver set heave displacement, the peak to peak amplitude displacement for PSS is 0.2082 m and for ASS is 0.004255 m. Peak to peak amplitude percentage reduction of ASS to PSS 97.9%. Settling time for ASS is 2 sec, whereas for PSS is 10 sec. settling time percentage reduction of ASS to PSS is 96.4 %. Therefore, the result show that the designed controller is significantly improves ride comfort and vehicle handling.

Conclusion

In this paper, modeling and control of a vehicle suspension system is addressed. The mathematical model for linear 8 DOF vehicle model suspensions systems using Lagrange equation has been formulated and derived. After the derivation of the dynamic model, a nonlinear control strategy (Second-order SMC) based on a super-twisting algorithm is designed and its performance is evaluated in three bump road disturbance inputs.

To verify the performance and efficiency of the controller, a simulation is done via MATLAB/Simulink. The results show that, the amplitude and settling time of sprung and unsprung masses heave displacements are extremely decreased in controlled ASS than uncontrolled PSS. Overall, the dynamic modeling and second-order SMC controller designed for the ASS is effective and has excellent performance.

References

[1] H. Pang, F. Liu, Z. Xu, Variable universe fuzzy control for vehicle semi-active suspension system with MR damper combining fuzzy neural network and particle swarm optimization, Neurocomputing. 306 (2018) 130–140. .

[2] H.O. Ozer, Y. Hacioglu, N. Yagiz, High Order Sliding Modes for Vehicle Suspensions Via, 1 (2016) 47–52.

[3] J.A. Tamboli, S.G. Joshi, Optimum design of a passive suspension system of a vehicle subjected to actual random road excitations, J. Sound Vib. 219 (1999) 193–205.

[4] Y. Shahid, M. Wei, Comparative analysis of different model-based controllers using active vehicle suspension system, Algorithms. 13 (2020).

[5] A. Ahmed, S.A. Ahmed, N.M. Ghazaly, G.T.A. el-Jaber, PID controller of active suspension system for a quarter car model, Int. J. Adv. Eng. Technol. 8 (2015) 899–909.

[6] Graduate Assistant Assistant Professor State University, (n.d.) 42–48.

[7] F. Hasbullah, W.F. Faris, A comparative Analysis of LQR and Fuzzy logic Controller for Active Suspension Using Half Car Model, (2010) 7–10.

[8] J. halim, S. bin, modeling and control of the active suspension system using proportional integral sliding mode approach yahaya md . sam and johari halim shah bin osman, 7 (2005) 91–98.

[9] T. Yoshimura, K. Nakaminami, M. Kurimoto, J. Hino, Active suspension of passenger cars using linear and fuzzy-logic controls, Control Eng. Pract. 7 (1999) 41–47.

[10] O. for, fpga based a daptive neuro fuzzy inference controller for f ull v ehicle, 1 (2010) 1–15.

[11] Z. Guosheng, Y. Song, Z. Xia, P. Jingyi, The Research of Automobile Suspension System Performance Based on the Fuzzy Neural Network Control, (2014) 1–6.

[12] J. Hyeon Park, Y. Suk Kim, An H ∞ Controlller for Active Suspensions and its Robustness Based on a

Full-Car Model, IFAC Proc. Vol. 32 (1999) 8178–8183.

[13] Reza N. Jazar, Vehicle Dynamics: Theory and Application, Springer Science+Business Media, LLC (2008)..

[14] Y. Shtessel, C. Edwards, L. Fridman, Sliding Mode Control and Observation, Series: Control Engineering, 2016.

Appendices A

Table 1. Specification of vehicle parameters used for simulation

Parameter	**Numerical value**
m_d	90 Kg
m_v	1161.9 kg
I_{xx}	398.4 kg m 2
I_{yy}	1872.4 kg m 2
m_f	95 kg
m_r	90 kg
k_d	16000 N/m
k_f	20040 N/m
k_r	24960 N/m
c_d	150 Ns/m
c_f	965 Ns/m
c_r	4000Ns/m
k_{tf}	177500 N/m
k_{tr}	177500 N/m
a, b	1.4m, 1.7 m
c, d	0.557m ,0.505 m respectively
e, f	1m, 0.25m respectively